Knock-Out of the Genes Coding for the Rieske Protein and the ATP-Synthase δ-Subunit of Arabidopsis. Effects on Photosynthesis, Thylakoid Protein Composition, and Nuclear Chloroplast Gene Expression[1][w]

Daniela Maiwald, Angela Dietzmann, Peter Jahns, Paolo Pesaresi, Pierre Joliot, Anne Joliot, Joshua Z. Levin, Francesco Salamini, and Dario Leister*

Abteilung für Pflanzenzüchtung und Ertragsphysiologie, Max-Planck-Institut für Züchtungsforschung, Carl-von-Linné-Weg 10, D–50829 Köln, Germany (D.M., A.D., P.P., F.S., D.L.); Institut für Biochemie der Pflanzen, Heinrich-Heine-Universität Düsseldorf, Universitätsstrasse 1, D–40225 Düsseldorf, Germany (P.J.); Institut de Biologie Physico-Chimique Service de Photosynthèse/Unité Propre de Recherche-Centre National de la Recherche Scientifique 1261, 13, rue Pierre et Marie Curie, 75005 Paris, France (P.J., A.J.); and Syngenta Biotechnology, Inc., 3054 Cornwallis Road, Research Triangle Park, North Carolina 27709 (J.Z.L.)

In Arabidopsis, the nuclear genes *PetC* and *AtpD* code for the Rieske protein of the cytochrome b_6/f (cyt b_6/f) complex and the δ-subunit of the chloroplast ATP synthase (cpATPase), respectively. Knock-out alleles for each of these loci have been identified. Greenhouse-grown *petc-2* and *atpd-1* mutants are seedling lethal, whereas heterotrophically propagated plants display a high-chlorophyll (Chl)-fluorescence phenotype, indicating that the products of *PetC* and *AtpD* are essential for photosynthesis. Additional effects of the mutations in axenic culture include altered leaf coloration and increased photosensitivity. Lack of the Rieske protein affects the stability of cyt b_6/f and influences the level of other thylakoid proteins, particularly those of photosystem II. In *petc-2*, linear electron flow is blocked, leading to an altered redox state of both the primary quinone acceptor Q_A in photosystem II and the reaction center Chl P700 in photosystem I. Absence of cpATPase-δ destabilizes the entire cpATPase complex, whereas residual accumulation of cyt b_6/f and of the photosystems still allows linear electron flow. In *atpd-1*, the increase in non-photochemical quenching of Chl fluorescence and a higher de-epoxidation state of xanthophyll cycle pigments under low light is compatible with a slower dissipation of the transthylakoid proton gradient. Further and clear differences between the two mutations are evident when mRNA expression profiles of nucleus-encoded chloroplast proteins are considered, suggesting that the physiological states conditioned by the two mutations trigger different modes of plastid signaling and nuclear response.

Plants use light energy to drive electron and proton transport across the thylakoid membrane, resulting in the synthesis of NADPH and ATP. These processes involve photosystems I (PSI) and II (PSII), cytochrome b_6/f (cyt b_6/f), and the chloroplast ATP synthase (cpATPase). During linear electron flow, cyt b_6/f accepts electrons from PSII and passes them via plastocyanin to PSI, thereby translocating protons across the thylakoid membrane into the lumen (Cramer et al., 1991). Additional protons accumulate in the thylakoid lumen due to the activity of the oxygen-evolving complex of PSII. The transthylakoid proton gradient serves both to drive the endergonic synthesis of ATP from ADP and orthophosphate (Kramer et al., 2003) and to regulate non-photochemical quenching of excitation energy (Muller et al., 2001).

In Arabidopsis, cyt b_6/f contains at least eight subunits, of which six are plastome-encoded; the nuclear genes *PetC* and *PetM* code for the Rieske iron-sulfur protein and subunit VII, respectively. Structure data imply a requirement of the Rieske protein for stability of cyt b_6/f: the trans-membrane helix of the iron-sulfur protein of the cytochrome b/c_1 complex cross-links the two monomers of the dimeric structure (Kim et al., 1998; Berry et al., 2000), and the [2Fe-2S] cluster-binding subdomains of the chloroplast and mitochondrial Rieske proteins are virtually identical (Carrell et al., 1997). To study the function of the major plastome-encoded proteins of cyt b_6/f, deletion strains for cytochrome *f* (cyt *f*), cytochrome b_6 (cyt b_6), and subunit IV (suIV) have been constructed in *Chlamydomonas reinhardtii*. The Δ*petA*, Δ*petB*, and Δ*petD* lines, which are unable to synthesize cyt *f*, cyt b_6, and suIV, respectively, can only be propagated heterotrophically (Kuras and Wollman, 1994). A *C. reinhardtii* line with a mutated *PetC* gene has also

[1] This work was supported by the European Community's Human Potential Program (contract no. HPRN–CT–2002–00248 [PSICO]), by the Deutsche Forschungsgemeinschaft (grant nos. DL 1265/1 and/8), and by the Bundesministerium für Bildung und Forschung (Förderkennzeichen 03117519).

[w] The online version of this article contains Web-only data.

* Corresponding author; e-mail leister@mpiz-koeln.mpg.de; fax 49–221–5062–413.

Article, publication date, and citation information can be found at www.plantphysiol.org/cgi/doi/10.1104/pp.103.024190.

been characterized (Lemaire et al., 1986; de Vitry et al., 1999). The mutant had no functional Rieske protein, resulting in complete suppression of photosynthetic electron flow. In Arabidopsis, the mutant *proton gradient regulation 1*, which is characterized by its lack of thermal dissipation of excitation energy, was shown to have a point mutation in *PetC* (Munekage et al., 2001). Although the rate of electron transport was not affected in *proton gradient regulation 1* under low light, it was significantly restricted under high-light fluence, supporting the conclusion that lumenal acidification was not sufficient to induce thermal dissipation.

Nine different polypeptides make up the cpATPase, which consists of the intrinsic CF_0 and the catalytic extrinsic CF_1 segments (Groth and Strotmann, 1999). As in the case of cyt b_6/f, most components of the cpATPase complex are plastome-encoded, and in Arabidopsis, only subunits b′, δ, and γ are encoded by the nuclear genes *AtpG*, *AtpD*, and *AtpC1/C2*, respectively. In *C. reinhardtii*, mutational analysis of plastome-encoded cpATPase polypeptides indicates that in the absence of assembly of the complex, the rate of synthesis of the β-subunit is controlled by the α-subunit (Lemaire and Wollman, 1989; Robertson et al., 1989). Furthermore, in the absence of cpATPase assembly, the thylakoid membranes of *C. reinhardtii* are devoid of CF_0, whereas α- and β-subunits, presumably constituting a soluble form of CF_1, accumulate in the stroma (Lemaire and Wollman, 1989). A *C. reinhardtii* line with an inactivated *AtpC* gene could only be propagated under heterotrophic conditions (Smart and Selman, 1991, 1993).

In this paper, we provide a molecular and physiological characterization of knock-out mutants for the Arabidopsis genes encoding the Rieske protein and the δ-subunit of the cpATPase. Both mutants cannot grow photoautotrophically, but the two mutations differ in their effects on the composition and redox state of the electron transport chain, as well as in their capacity for electron and proton transport. Analysis of the expression of nuclear chloroplast genes indicates that the two mutations trigger different plastid-to-nucleus signaling pathways.

RESULTS

Identification of Mutant Alleles of the *PetC* and *AtpD* Genes

The mutant *petc-1* (*PetC*::*En1*), which has an *En* transposon inserted in the fourth intron of the *PetC* gene, was identified by PCR screening of transposon-mutagenized Arabidopsis ecotype Columbia 0 (Col-0) lines (Wisman et al., 1998; Fig. 1a). In addition, a phenotypic screen of Arabidopsis lines of the ecotype Landsberg *erecta* (L*er*) mutagenized with the *Ds* transposon led to the identification of the seedling-lethal line GT1802 carrying an insertion at

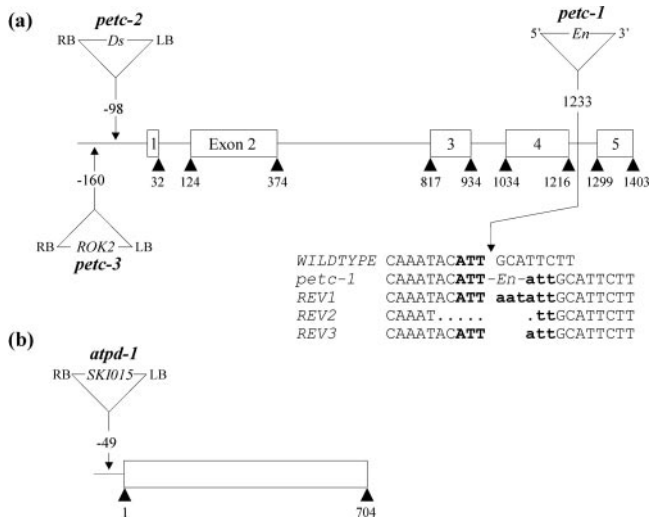

Figure 1. Mutations in the *PetC* and *AtpD* loci. a, In *petc-1*, the *PetC* gene (At4g03280) is disrupted by an insertion of the autonomous *En* transposon. The sequences of the empty donor sites of DNA from three independent somatic revertant leaves (REV1–3) were obtained by PCR; uppercase letters indicate plant DNA sequences flanking the *En*; insertion footprints left at each locus after *En* transposition are indicated by bold lowercase letters; and bold uppercase letters indicate the target site in the WT. In the other two mutant alleles, a copy of the nonautonomous *Ds* transposon (*petc-2*) and the ROK2 T-DNA (*petc-3*) are inserted 5′ of the start codon of the *PetC* gene. b, In *atpd-1*, a copy of the 5.2-kb SKI015 T-DNA is inserted in the promoter region of *AtpD* (At4g09650). PCR analysis indicated a small deletion of 7 bp adjacent to the right border of the *SKI015* insertion. The *En*, *Ds*, and T-DNA insertions are not drawn to scale.

the *PetC* locus (Budziszewski et al., 2001). This line, designated *petc-2*, contains a *Ds* insertion 98 bp upstream of the ATG of *PetC* (Fig. 1a). A third *petc* allele was identified when the insertion flanking database SIGnAL (http://signal.salk.edu/cgi-bin/tdnaexpress) was searched for insertions at the *PetC* locus. This line (ecotype Col-0) had a copy of the 5.2-kb pROK2 T-DNA inserted 160 bp 5′ to the ATG of the *PetC* gene and was designated *petc-3* (Fig. 1a).

In the course of the phenotypic screen carried out by Budziszewski et al. (2001; see above), the seedling-lethal line 4144 (ecotype Col-0) with an SKI015 T-DNA insertion at the *AtpD* locus was identified. In this line, designated *atpd-1*, the T-DNA is located 49 bp upstream of the ATG of *AtpD* (Fig. 1b).

PetC and *AtpD* Are Essential for Photosynthesis

When grown on soil, all three *petc* mutants germinated, but their seedlings exhibited a yellowish pigmentation of cotyledons and were not capable of autotrophic growth. Crosses between heterozygous *petc-1*, *-2*, and *-3* plants resulted in F_1 progenies segregating with a 3:1 ratio of wild type (WT) to mutant, demonstrating that the three mutations were allelic. All three *petc* alleles could be propagated in sterile culture on Murashige and Skoog medium supple-

mented with sucrose. In axenic culture, *petc* plants had a light-green leaf coloration and exhibited a substantially reduced growth rate compared with WT plants (Fig. 2a). The pigment deficiency was less severe under low light (12 μmol photons s^{-1} m^{-2}) than under higher light conditions (70 μmol photons s^{-1} m^{-2}), indicating enhanced photosensitivity of the mutants (data not shown). The *petc-1* mutant displayed somatic reversions to WT due to the excision of the *En* transposon. In each such WT sector, empty donor sites could be amplified by PCR, and these results therefore confirm the tagging of the gene (Fig. 1a). Of the three *petc* alleles available, *petc-2* was used for all further analyses. Upon illumination with UV-light, *petc-2* showed high-chlorophyll (Chl) fluorescence, indicating a block in photosynthetic electron flow (Fig. 2b). This phenotype is reminiscent of that of tobacco (*Nicotiana tabacum*) mutants with disrupted chloroplast *petA*, *petB*, or *petD* genes, all of which lack a functional cyt b_6/f complex (Monde et al., 2000).

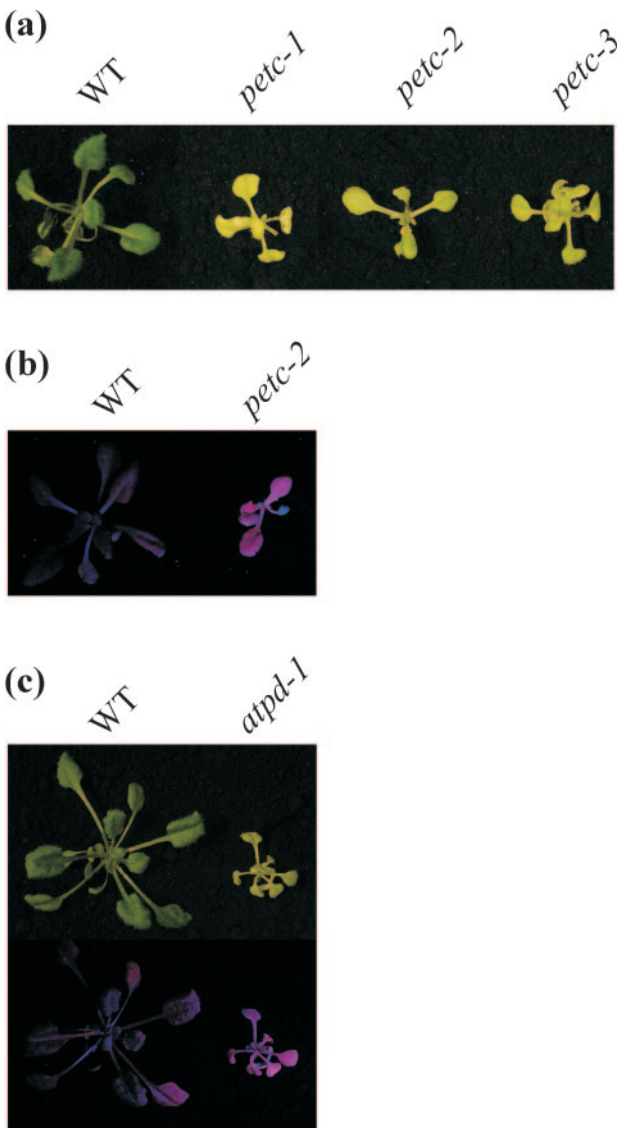

Figure 2. Phenotypes of WT, *petc*, and *atpd* plants. Plants grown on Murashige and Skoog medium supplemented with Suc were illuminated with white light or UV light (B-100AP/R, UVP Inc., Upland, CA). a, WT and *petc-1*, *-2*, and *-3* plants illuminated with white light; b, WT and *petc-2* plants under UV light; and c, WT and *atpd-1* plants under white light (top) or UV light (bottom).

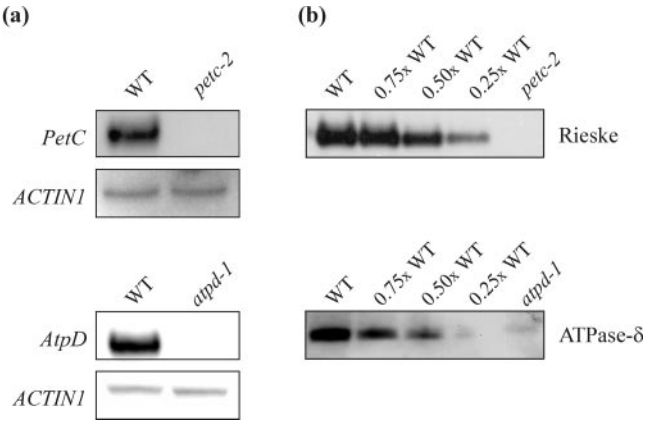

Figure 3. *AtpD* and *PetC* mRNA and protein levels in WT and mutant plants. a, For northern analysis of the *PetC* transcript in *petc-2* and WT plants, 30-μg samples of total RNA were analyzed using a fragment of the *PetC* transcript as a probe. A full-length *AtpD* cDNA was used as a probe for northern analysis of the *AtpD* transcript in *atpd-1* and WT plants. As a loading control, the blots were reprobed with a cDNA fragment derived from the *ACTIN1* gene. b, Samples of thylakoid membranes equivalent to 5 μg of Chl from WT and *petc-2* or *atpd-1* plants were fractionated by denaturing PAGE. Decreasing amounts of WT thylakoid membranes (3.75, 2.5, and 1.25 μg of Chl) were loaded in the lanes marked 0.75×, 0.5×, and 0.25× WT. Filters were probed with antibodies specific for the Rieske protein or the δ−subunit of the cpATPase.

Like the *petc* mutants, greenhouse-grown *atpd-1* plants displayed a seedling-lethal and pigment-deficient phenotype. When grown heterotrophically, the *atpd-1* mutant grew more slowly than the WT, displaying light-green leaf coloration and an high-Chl fluorescence phenotype (Fig. 2c). By complementing *atpd-1* mutant plants with the *AtpD* cDNA under the control of the 35S promoter, WT-like growth and leaf coloration was restored, demonstrating that the *atpd-1* phenotype was due to a lack of *AtpD* function (data not shown).

Expression of *PetC* and *AtpD* Transcripts and Proteins in the Mutants

Northern analysis of *petc-2* plants using a *PetC*-specific probe revealed that the expression of the *PetC* transcript was drastically reduced by the *Ds* insertion. In *atpd-1* plants, a similar effect of the T-DNA insertion on *AtpD* mRNA accumulation was detected (Fig. 3a). Western analyses demonstrated the absence of detectable amounts of the Rieske protein in *petc-2* thylakoids and of cpATPase-δ in *atpd-1* thylakoids (Fig. 3b).

Leaf Pigments and Thylakoid Multiprotein Complexes

WT, *atpd-1*, and *petc-2* plants growing in axenic culture were analyzed for leaf pigment and thylakoid protein content. In both mutants, the total Chl concentration (Chl *a* + *b*) was drastically reduced, which is consistent with the light-green coloration of leaves. The Chl *a*/*b* ratio was decreased in *petc-2* and to a much greater extent in *atpd-1* plants (Table I), indicating substantial changes in photosystem composition and/or stoichiometry. The markedly increased xanthophyll content and the reduced β-carotene level (relative to Chl *a* + *b*) in both mutants indicate an increased accumulation of antenna proteins in relation to reaction center core proteins (Table I). The disproportionate increase in the size of the VAZ pool can be interpreted as a consequence of the higher photosensitivity in both mutant lines. Moreover, the high de-epoxidation state of the VAZ pool detected in *atpd-1* plants, but not in the *petc-2* mutant, points to a sustained increase in the transmembrane proton gradient in *atpd-1*, leading to activation of violaxanthin de-epoxidase even under low light intensities (12 μmol photons m^{-2} s^{-1}).

The relative enrichment of antenna proteins in the two mutants was supported by analyses of the protein composition of thylakoid membranes either by two-dimensional PAGE or by western analysis after one-dimensional PAGE. For two-dimensional PAGE, thylakoid samples equivalent to 30 μg of Chl were fractionated, and protein spots were assigned to individual subunits of the photosynthetic apparatus according to Pesaresi et al. (2001) and Grasses et al. (2002; Fig. 4a). For one-dimensional PAGE analysis, protein amounts equivalent to 5 μg of Chl were loaded and fractionated for each genotype and after transfer to membranes, were incubated with antibodies specific for individual thylakoid polypeptides (Fig. 4, b and c). Densitometric analyses of two-dimensional protein gels revealed that in *petc-2* plants, the abundance of the core proteins of PSII and of PSI was substantially decreased (to 14% and 34% of WT levels per gram of fresh leaf weight, respectively), whereas the level of antenna proteins of both photosystems (LHCII and Lhca4) decreased only to about 35% to 40% of WT, which would be consistent with a preferential loss of PSII core proteins (Table I). Similarly, in *atpd-1* plants, the relative abundance of PSII and PSI core proteins was significantly lower than that of the respective antenna proteins. However, in contrast to the case in *petc-2* plants, in *atpd-1*, the relative level of PSI core proteins was more drastically reduced. Because PSI core proteins bind more Chl *a* than PSII core proteins, the disproportionate reduction of PSI in *atpd-1* explains the extremely low Chl *a*/*b* ratio recorded for this mutant (Table I). As expected, the α + β-subunits of the cpATPase did not

Table I. *Leaf pigments and thylakoid proteins in petc-2, atpd-1, and WT plants*

The pigment content of WT and mutant plants ($n = 5$ each) was determined by HPLC. Total Chl content is given in nanomoles of Chl (*a* + *b*) per gram fresh weight. The carotenoid content is expressed as millimoles per mol of Chl (*a* + *b*). Mean values (±SD) are shown. Nx, Neoxanthin; β-Car, β-carotene; VAZ, sum of the xanthophyll cycle pigments (violaxanthin + antheraxanthin + zeaxanthin); DEPS, de-epoxidation state = (violaxanthin + 0.5 antheraxanthin) / (violaxanthin + antheraxanthin + zeaxanthin). Values for proteins are average optical densities (±SD) measured from three independent two-dimensional protein gel analyses (PSII core, OEC, PSI, ATPase (α + β), and LHCII; see also Fig. 4a) or from three independent Western analyses (PSII-D1, PSI-F, ATPase (α + β)*, cyt b_6, cyt *f*, suIV, and Lhca4; see also Fig. 4, b and c). The relative values for the two mutant genotypes, reported in columns 4 and 7, reflect the ratio of expression between the mutant and WT from the same amount of fresh weight tissue. This correction was performed using the measured levels of total Chl content. nd, Not determined.

Pigment/Protein	L*er*	*petc-2*	Relative Level in *petc-2*	Col-0	*atpd-1*	Relative Level in *atpd-1*
			% of WT			*% of WT*
Chl *a*/*b*	3.04 ± 0.03	2.72 ± 0.07		3.02 ± 0.07	2.24 ± 0.06	
Chl *a* + *b*	1,900 ± 33	845 ± 24	44	1,999 ± 40	894 ± 11	45
Lutein	123 ± 3	164 ± 7	59	129 ± 4	144 ± 1	50
Nx	36 ± 2	44 ± 3	54	35 ± 1	46 ± 3	59
VAZ	27 ± 1	65 ± 5	106	25 ± 3	95 ± 6	171
β-Car	70 ± 2	59 ± 3	37	71 ± 7	32 ± 5	20
DEPS	0.03 ± 0.01	0.08 ± 0.01		0	0.30 ± 0.02	
PSII core	4.93 ± 0.32	1.52 ± 0.30	14	3.94 ± 0.04	2.55 ± 0.30	29
PSII-D1	1.76 ± 0.13	0.18 ± 0.02	5	1.10 ± 0.13	0.47 ± 0.06	19
OEC	0.97 ± 0.01	0.36 ± 0.02	16	1.83 ± 0.03	0.76 ± 0.02	19
PSI	2.77 ± 0.17	2.11 ± 0.35	34	3.33 ± 0.07	1.23 ± 0.06	17
PSI-F	1.10 ± 0.12	1.15 ± 0.06	46	0.75 ± 0.07	0.31 ± 0.04	19
ATPase (α+β)	2.92 ± 0.25	3.87 ± 0.27	58	1.58 ± 0.10	0	0
ATPase (α+β)*	0.71 ± 0.05	1.02 ± 0.02	63	1.51 ± 0.12	0	0
Rieske	1.38 ± 0.15	0	0	1.73 ± 0.12	1.12 ± 0.07	29
cyt b_6	1.34 ± 0.46	0.12 ± 0.01	4	1.63 ± 0.01	0.84 ± 0.00	23
cyt *f*	2.15 ± 0.11	2.23 ± 0.09	46	nd	nd	nd
suIV	1.47 ± 0.06	0.95 ± 0.03	28	nd	nd	nd
LHCII	8.07 ± 0.30	6.88 ± 0.13	38	10.64 ± 0.25	10.30 ± 0.36	44
Lhca4	2.10 ± 0.08	1.66 ± 0.11	35	2.25 ± 0.18	1.83 ± 0.12	37

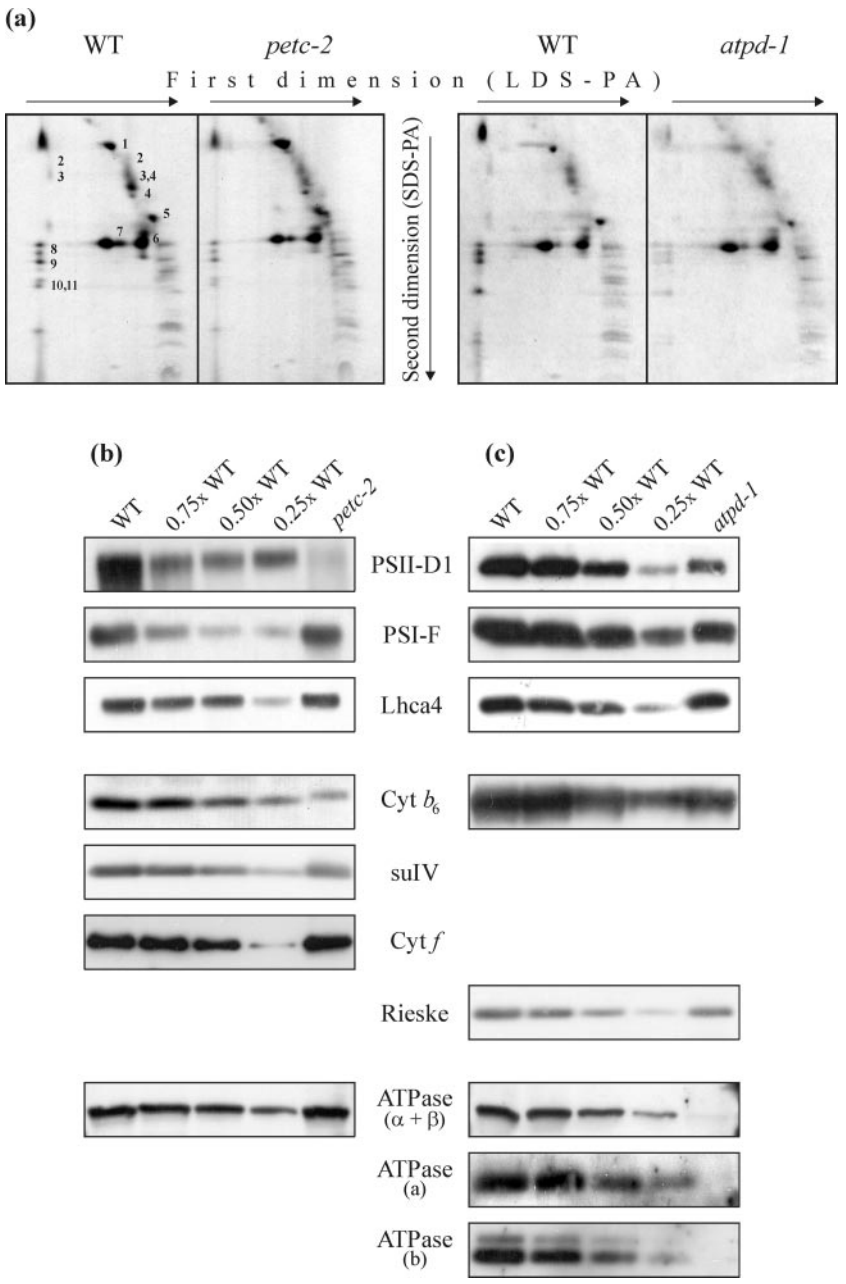

Figure 4. Protein composition of thylakoid membranes. a, Thylakoid membranes corresponding to 30 μg of Chl from WT, *petc-2*, and *atpd-1* mutant plants were fractionated first by electrophoresis on a non-denaturing lithium dodecyl sulfate-polyacrylamide (PA) gel and then on a denaturing SDS-PA gel. Positions of WT thylakoid proteins previously identified by western analyses with appropriate antibodies are indicated by numbers to the right of the corresponding spots: 1, α- and β-subunits of the ATPase complex; 2, D1-D2 dimers; 3, CP47; 4, CP43; 5, oxygen-evolving complex (OEC); 6, LHCII monomer; 7, LHCII trimer; 8, PSI-D; 9, PSI-F; 10, PSI-C; and 11, PSI-H. The alterations observed in the mutants are quantified in Table I. Samples of thylakoid membranes equivalent to 5 μg of Chl from WT, and *petc-2* (b) and *atpd-1* (c) plants were fractionated by denaturing PAGE. Decreasing amounts of WT thylakoid membranes (3.75, 2.5, and 1.25 μg of Chl) were loaded in the lanes marked 0.75×, 0.5×, and 0.25× WT. Replicate filters were probed with antibodies raised against the D1 protein of the PSII reaction center, the F subunit of PSI, the Lhca4 protein, the cyt b_6/f subunits cyt b_6, cyt *f* and suIV, and the α-, β-, a-, and b-subunits of the cpATPase.

accumulate to detectable amounts in *atpd-1* plants (Fig. 4c), indicating a destabilization of the CF_1 complex in this mutant (see above), whereas the complex was present at about 60% of WT levels in *petc-2* (Fig. 4b). Moreover, absence of the CF_1 protein ATPase-δ appears also to destabilize the CF_0 complex, because no accumulation of the CF_0-a and -b proteins was detected in *atpd-1* (Fig. 4c).

Western analysis of thylakoid proteins separated by denaturing one-dimensional PAGE with specific antibodies showed that the relative decrease in the level of the D1 protein in *petc-2* exceeded that of the entire PSII core (Fig. 4b; Table I). This strong reduction in D1 levels could be explained by enhanced destabilization of the D1 protein due to increased photoinhibition in mutant plants. Western analysis with Rieske- and cyt b_6-specific antibodies revealed that in *atpd-1* the level of cyt b_6/f decreased stoichiometrically with PSI and PSII concentrations. In contrast, in *petc-2*, an almost complete absence of cyt b_6 was evident, whereas residual cyt *f* and suIV levels of about 50% and 30%, respectively, of WT were detected (Fig. 4b; Table I), suggesting that cyt *f* and suIV can accumulate in the absence of the Rieske and cyt b_6 proteins. This is in contrast to previous analyses carried out in maize (*Zea mays*; Miles, 1982), *Oenothera* sp. (Stubbe and Herrmann, 1982), and *Lemna* sp. (Bruce and Malkin, 1991) mutants defective in the

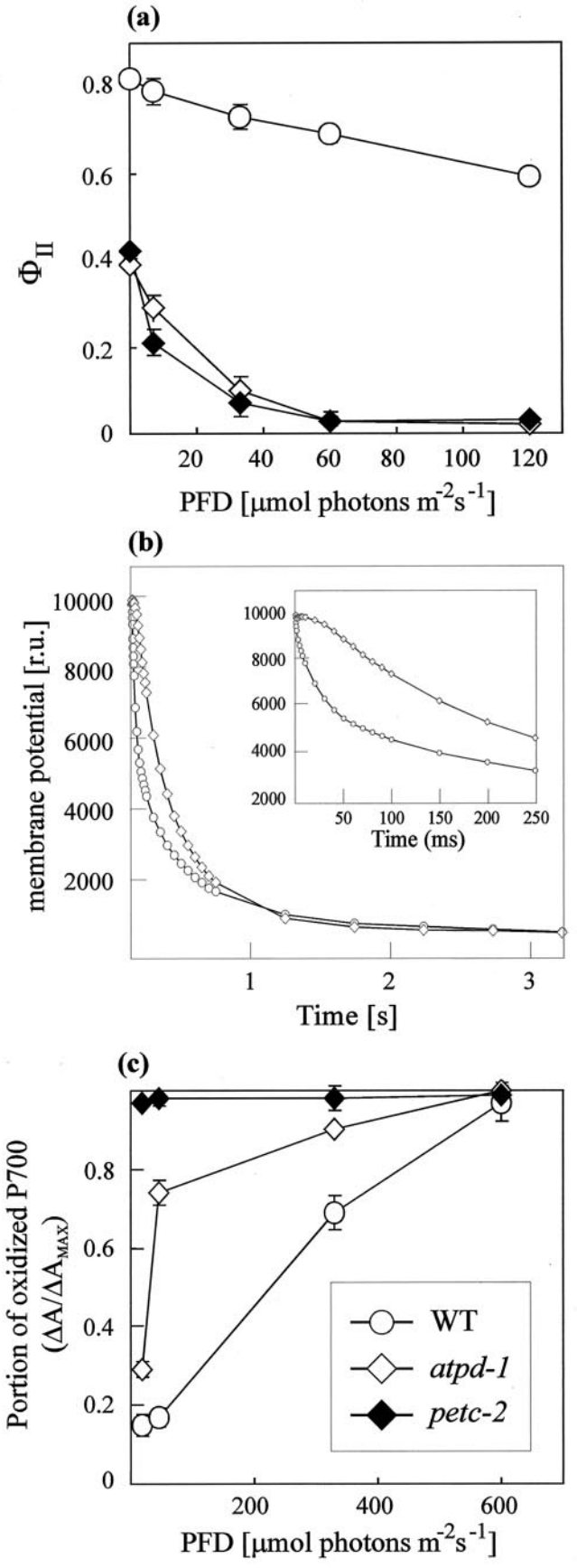

assembly of cyt b_6/f, which led to the conclusion that the Rieske protein is essential for the assembly of the cyt b_6/f complex (Bruce and Malkin, 1991). Instead—similar to the situation in *C. reinhardtii* (Lemaire et al., 1986; de Vitry et al., 1999)—in Arabidopsis thylakoids, some cyt b_6/f proteins accumulate in the absence of the Rieske protein.

Functional Photosystems Exist in Both Mutants But Only *atpd-1* Shows Linear Electron Transport Activity

PSII fluorescence parameters, thylakoid membrane potential decay, and the oxidation state of P700 under continuous illumination were determined (Table II; Fig. 5). The maximum quantum yield of PSII (F_v/F_m) was substantially reduced in both mutants, indicating the presence of inactive PSII centers. Moreover, in *petc-2* and *atpd-1*, the strong reduction in the effective quantum yield of PSII, Φ_{II} (Table II), and the pronounced decrease of Φ_{II} with increasing light intensities (Fig. 5a) implies a severe perturbation of electron flow, which is consistent with the high photosensitivity of the mutants. The dramatically increased fraction of reduced Q_A (1-qP) in *petc-2* (Table II), on the other hand, can be explained by the blockade of electron transport through cyt b_6/f. The extent of non-photochemical fluorescence quenching (NPQ) at a photon flux density (PFD) of 12 µmol photons m^{-2} s^{-1} revealed the absence of NPQ in *petc-2*, but significantly increased thermal energy dissipation in *atpd-1* (Table II). The strong increase in NPQ in *atpd-1* plants at this low light intensity strongly suggested an increase in acidification of the thylakoid lumen, because the major portion of NPQ is related to the ΔpH-dependent component (qE). An increase in lumen acidification is consistent with the high deepoxidation state in *atpd-1* (see above and Table I) and can be related to the loss of cpATPase function in this genotype. To clarify this aspect, the thylakoid membrane potential decay was analyzed in WT and *atpd-1* leaves (Fig. 5b). As described previously by

Figure 5. Spectroscopic analyses of WT, *petc-2*, and *atpd-1* plants. a, Effective quantum yield of PSII (Φ_{II}) in leaves of *atpd-1*, *petc-2*, and WT plants determined at different photon flux densities. Leaves were dark-adapted for 30 min before the measurements were made. Mean values of five independent experiments are shown. Bars indicate SDs. b, Thylakoid membrane potential decay of WT and *atpd-1* leaves. Maximum transthylakoid proton gradient was reached by exposing 4-week-old leaves of WT and *atpd-1* plants to a saturating light pulse for 15 and 25 ms, respectively. The dark-induced thylakoid membrane potential decay was then monitored by recording the absorption at 520 nm. For the absorption measurements, short light pulses at 520 nm were used to prevent actinic effects. The results of one out of five measurements are shown. c, Steady-state levels of oxidized reaction center Chl in PSI ($P700^+$) in WT and mutant plants ($n = 3$ each). The steady-state level of $P700^+$ was measured from the change in P700 absorption at 820 nm ($\Delta A/\Delta A_{MAX}$) after 5 min of illumination with actinic light. Mean values are shown, and bars indicate SDs.

Table II. *Spectroscopic analysis of WT, petc-2,* and *atpd-1* plants ($n = 5$ each). Mean values (±SD) are shown. F_v/F_m, maximum quantum yield of PSII; Φ_{II}, effective quantum yield of PSII; 1-qP, fraction of Q_A (the primary electron acceptor of PSII) present in the reduced state; NPQ, non-photochemical quenching. Values for WT plants were identical for both ecotypes, Col-0 and L*er*.

Parameter	WT	*petc-2*	*atpd-1*
F_v/F_m	0.82 ± 0.01	0.42 ± 0.01	0.39 ± 0.01
Φ_{II}	0.77 ± 0.01	0.16 ± 0.02	0.23 ± 0.02
1-qP	0.04 ± 0.01	0.81 ± 0.02	0.14 ± 0.06
NPQ	0.07 ± 0.01	0.01 ± 0.00	0.26 ± 0.03

Junge et al. (1970), WT leaves showed a biphasic thylakoid membrane potential decay: a fast phase, completed in approximately 100 ms (see detail in Fig. 5b), ascribed to cpATPase activity; and a slow phase, completed in approximately 3 s, ascribed to ions leaks through the membrane. In *atpd-1* leaves, the fast decaying phase was absent, and only a slow monophasic thylakoid membrane potential decay completed in about 3 s was observed, clearly suggesting a specific inhibition of cpATPase function.

The oxidation state of P700 in intact leaves at various actinic light intensities was determined by measuring the absorbance changes at 820 nm (Fig. 5c). In comparison with WT, maximum oxidation of P700 was reached at much lower PFDs in *atpd-1*, indicating that electron transport was saturated at lower light intensities in this mutant. In contrast, in *petc-2* plants, P700 was fully oxidized even at the lowest light intensities used, implying that electron transport to PSI is completely blocked in the absence of the Rieske protein.

Similar conclusions can be drawn from the comparison of electron transport rates determined in isolated thylakoids. Using artificial electron acceptors and/or donors, activity of both photosystems was recorded in thylakoids from all types of plants, indicating that functional PSI and PSII complexes still exist in the two mutants (Table III). Linear electron flow, however, was only detectable in *atpd-1*, demonstrating again that the absence of the Rieske protein in *petc-2* completely suppresses electron transport through cyt b_6/f.

The results presented are consistent with a block in linear electron flow, over-reduction of the plastoquinone pool, and a decrease in the transthylakoid pH gradient in *petc-2*. However, in *atpd-1*, electron flow is impaired but not completely blocked. Due to the suppression of proton flow through the cpATPase, electron flow is saturated at significantly lower light intensities, resulting in an increase in lumen acidification and thermal energy dissipation under low light. The phenotypes of each of the Arabidopsis knock-out mutants are more severe than those of tobacco *PetC* and *AtpD* antisense lines (Price et al., 1995) or those of Arabidopsis plants with a point mutation in the Rieske protein (Munekage et al., 2001; Jahns et al., 2002), but in general, they show similar trends.

Expression of mRNAs for Nucleus-Encoded Chloroplast Proteins in the Mutants

The data discussed above show that the lack of either the Rieske protein (*petc-2*) or the δ-subunit of the cpATPase (*atpd-1*) completely suppresses photosynthesis, leading to seedling lethality. However, the two mutations have quite different effects on electron flow and the composition of thylakoids. To test for further differences in photosynthetic and other chloroplast functions, the expression levels of nuclear genes that contribute to chloroplast function were determined at the mRNA level in both mutants by DNA array analysis. This was carried out on a set of 3,292 nuclear genes, 81% of which code for chloroplast-targeted proteins, and their expression patterns in *petc-2* and *atpd-1* mutants were compared with those in WT, as done by Kurth et al. (2002) and Richly et al. (2003). The *psae1-1*, *psad1-1*, *psan-1*, and *psao-1* lines (Varotto et al., 2000; Richly et al., 2003; D. Leister, unpublished data) bearing knock-out alleles of the PSI genes *PsaE1*, *PsaD1*, *PsaN*, and *PsaO* were included as additional controls. In all six mutant ge-

Table III. *Activity of PSII and PSI and the rate of uncoupled linear electron transport in WT, petc-2,* and *atpd-1* thylakoids

Values of average oxygen evolution (PSII activity and linear electron transport) or consumption (PSI activity; ±SD) in micromoles of O_2 per milligram of Chl per hour were derived from three independent measurements of thylakoids equivalent to 10 μg of Chl per milliliter. The relative values for the two mutant genotypes, provided in columns 4 and 6, reflect the ratio of activity between the mutant and WT from the same amount of fresh weight tissue. Because average rates of oxygen evolution/consumption of thylakoids from WT plants of both ecotypes, Col-0 and L*er*, were very similar, only Col-0 values are shown.

Parameter	WT	*petc-2*	Relative Level in *petc-2*	*atpd-1*	Relative level in *atpd-1*
			%		%
PSII activity	134 ± 7	12 ± 0	3.9	84 ± 7	28
PSI activity	151 ± 7	251 ± 8	73	88 ± 7	26
Linear electron transport (uncoupled)	84 ± 7	0 ± 0	0	54 ± 2	29

notypes, we identified a set of 344 genes that were expressed at significantly different levels from WT in at least five of the six genotypes. Hierarchical clustering of the 344 gene expression profiles revealed that the expression patterns of the *petc-2* and *atpd-1* mutants were substantially different: The *petc-2* profile was related to that of *psae1-1* and *psad1-1*, whereas the pattern of *atpd-1* was more similar to that of *psan-1* or *psao-1* (Fig. 6a; supplementary material 1).

Direct comparison of the differential expression profiles of *petc-2* and *atpd-1* plants revealed that among all genes differentially expressed in the two genotypes, 451 genes showed the same trend (379 up- and 72 down-regulated). A further set of 346 genes showed opposite trends in transcriptional regulation in the two lines: 49 genes were up-regulated in *petc-2* and down-regulated in *atpd-1*, whereas 297 genes were down-regulated in *petc-2* but up-regulated in *atpd-1* (supplementary material 2).

The differentially expressed genes in *petc-2* and *atpd-1* were grouped into seven major functional categories, including metabolism, photosynthesis, transport, protein phosphorylation, stress response, transcription and translation, and unclassified proteins (Fig. 6b; supplementary material 3). In *petc-2*, a balanced response of the nuclear chloroplast transcriptome was observed, with about equal fractions of genes being up- or down-regulated (632 and 528 genes, respectively). Relatively more genes for photosynthesis tended to be down-regulated, whereas genes for stress response represented the largest up-regulated group of genes in this genotype. In contrast, in the *atpd-1* mutant, 88% of the differentially regulated genes were up-regulated. Most of the different functional gene classes followed this trend, again with the exception of genes coding for proteins involved in photosynthesis (only 27% of which were up-regulated).

The results show that the *petc-2* and *atpd-1* mutations result—with the exception of photosynthetic genes, which are predominantly down-regulated in both genotypes—in very different transcriptional responses of the nuclear chloroplast transcriptome. One possible explanation is that different types of plastid signaling pathways (Surpin et al., 2002; Pfannschmidt, 2003) are triggered by the physiological effects of the two mutations. Because the reduction state of Q_A, the primary electron acceptor of PSII, is in fact substantially increased in *petc-2* and *psad-1* (this study) and in *psae1-1* (Varotto et al., 2000) but not in *atpd-1* and *psao-1* (this study) or in PSI-N mutants (Haldrup et al., 1999), the different redox state of thylakoids in the two mutants could be responsible for the different transcriptional responses. A second possibility is that the different levels of lumenal acidification in the two mutants are sensed and signaled to the nucleus, resulting in different responses.

DISCUSSION

The Rieske Protein

Our results indicate that in Arabidopsis, diminished amounts of cyt *f* and suIV can accumulate in the absence of the Rieske protein. This is somewhat in contrast to the conclusion of previous analyses (Miles, 1982; Stubbe and Herrmann, 1982; Bruce and Malkin, 1991) that in flowering plants the Rieske protein is necessary for normal accumulation of cyt b_6/f. Bruce and Malkin (1991) proposed an "all-or-none" mechanism in which all major cyt b_6/f proteins must be present for the stable assembly of the complex. However, in the *petc-2* mutant of Arabidopsis, accumulation of the Rieske protein and of cyt b_6 are concomitantly impaired; this is a much stronger phenotype than the one observed in *C. reinhardtii petc* mutants, in which all of the cyt b_6, cyt *f*, and suIV proteins accumulate to about 60% of WT levels (de Vitry et al., 1999).

The lack of functional cyt b_6/f led to a markedly altered thylakoid protein composition. Only little functional PSII was detectable, indicating either that (a) in WT thylakoids PSII and cyt b_6/f physically interact or, more likely, that (b) the over-reduced plastoquinone pool leads to an increase in damage and degradation of PSII proteins, or that (c) transcription and/or translation of PSII subunits is secondarily down-regulated as a consequence of the drastically altered redox state (see Table II) in mutant thylakoids. In *petc-2*, the cpATPase accumulated to about 60% of WT levels. This could indicate that a transthylakoid pH gradient is maintained by the ATPase activity of the cpATPase (under ATP consumption) to facilitate ΔpH-dependent energy quenching, as well as the import of thylakoid proteins by the ΔpH-dependent twin-Arg translocation (Tat) pathway (Robinson et al., 2001).

The cpATPase-δ Protein

The δ-subunit of the cpATPase is thought to be located at the top region of the $\alpha_3\beta_3$ hexagon of the CF_1 component, connected with the extramembranous domains of the subunits b and b′ (Lill et al., 1996) with which it should form a stator in the rotatory machinery of F_0F_1 (Böttcher et al., 1998; Engelbrecht et al., 1998). Mutational analyses of the homologs of cpATPase-δ in *Escherichia coli* (Hazard and Senior, 1994a, 1994b; Stack and Cain, 1994) or yeast (Prescott et al., 1994; Straffon et al., 1998) indicate that the protein is essential for the function of the ATPase complex.

Our results indicate that in *atpd-1* plants, the photosystems, cyt b_6/f, and thus linear electron flow are still functional, whereas both the CF_0 and CF_1 component of the cpATPase are missing. Because the transthylakoid protein gradient cannot be used to drive ATP synthesis, increased acidification of the lumen

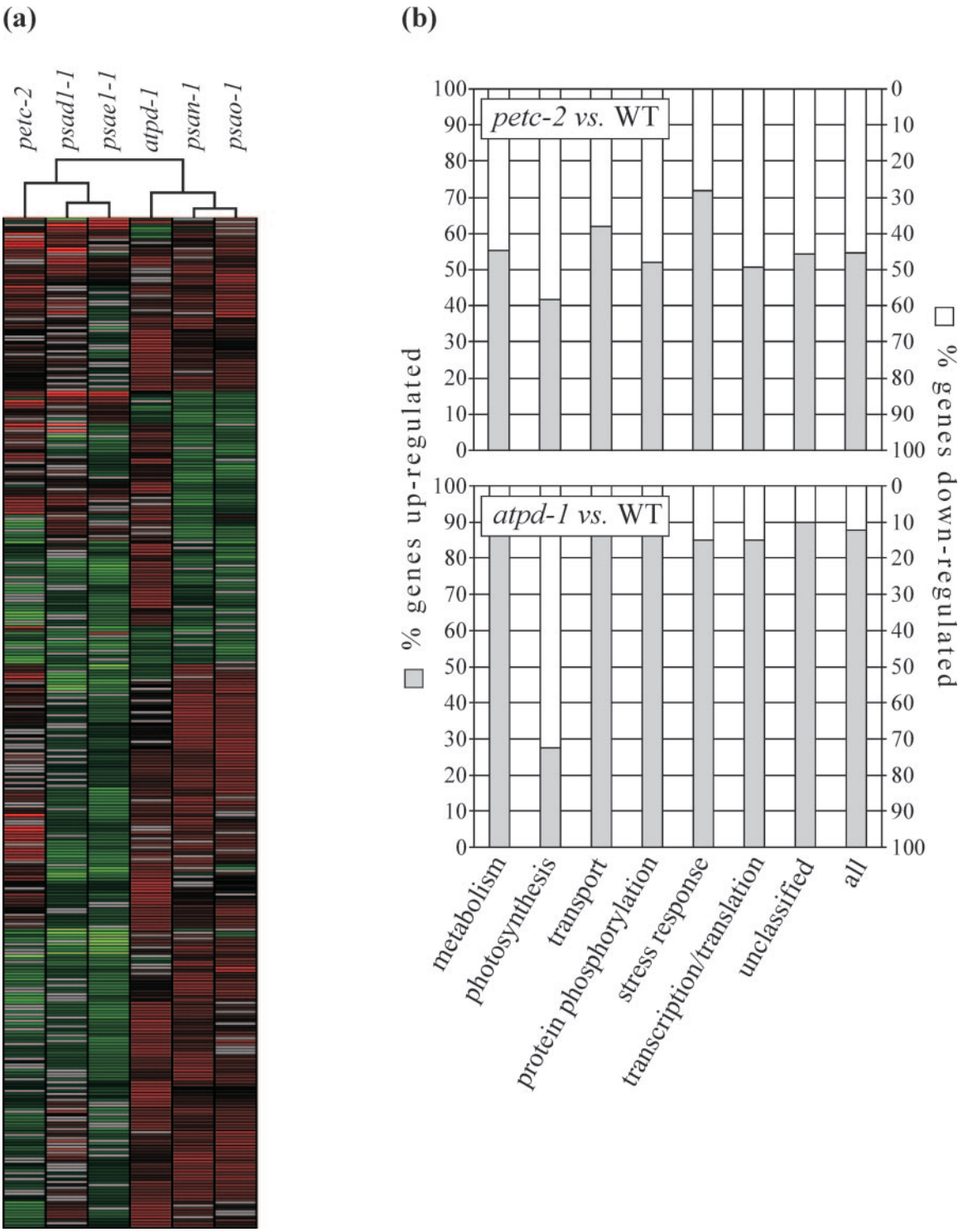

Figure 6. Effects of *petc-2* and *atpd-1* mutations on the accumulation of nuclear transcripts encoding chloroplast proteins. a, Hierarchical clustering of the expression profiles of 344 genes that show significant differential expression in at least five of the six mutants *petc-2*, *atpd-1*, *psae1-1*, *psad1-1*, *psan-1*, and *psao-1*. The cladogram at the top summarizes the degree of relatedness between transcriptome responses. Colors indicate up-regulation (red) or down-regulation (green) of gene expression relative to WT. Gray lines indicate non-significant differential expression. For a more detailed image, including gene accession numbers and annotations, see supplementary material 1. b, Fraction of up- and down-regulated genes in seven major functional categories. A complete list of significantly differentially expressed genes is available as supplementary material 3.

should lead to an increased non-photochemical quenching of excitation energy at low light intensities.

Thylakoid Composition and Plastid Signaling

Both the Rieske protein and the δ-subunit of the cpATPase are essential for photosynthesis. Absence of either of the two proteins causes loss of photoautotrophy and increased photosensitivity and affects accumulation of other thylakoid proteins. A closer inspection of our results allows recognition that leaf pigment and thylakoid composition are markedly different in the two genotypes. In *petc-2*, the plastoquinone pool is substantially over-reduced, whereas the almost complete suppression of NPQ indicates a decrease in thylakoid lumen acidification. On the contrary, *atpd-1* plants exhibit markedly increased NPQ, which is consistent with a slower dissipation of the transthylakoid proton gradient.

The majority of chloroplast proteins are encoded in the nucleus (Abdallah et al., 2000), making a communication between the two organelles necessary. Intermediates of the tetrapyrrole biosynthetic pathway (Strand et al., 2003), as well as the redox state of the photosynthetic apparatus (Pfannschmidt, 2003), have been associated with the generation of the so-called plastid signal which results in the modulation of the transcription of nuclear-encoded chloroplast proteins. Furthermore, because the transthylakoid proton gradient serves both to drive the endergonic synthesis of ATP from ADP and orthophosphate (Kramer et al., 2003) and to initiate non-photochemical quenching of excitation energy (Muller et al., 2001), it can be expected that changes in the pH gradient will, at least indirectly, produce a signal that modulates nuclear transcription of chloroplast protein genes. In this study, the expression profiling of more than 3,000 nuclear genes, most of them coding for chloroplast functions, showed that apart from the down-regulation of the majority of photosynthetic genes in both genotypes, different transcriptional responses were induced by the two mutations. Because photosynthesis was abolished in both genotypes, many secondary effects due to loss of photoautotrophy should be similar in the mutants. This allows the conclusion that many, if not most, differences in the expression profile of *petc-2* and *atpd-1* should be due to the different signaling function of changes in transthylakoid proton gradient and/or the redox state of the photosynthetic machinery.

Outlook

It is obvious that the concomitant lack of additional subunits of the cyt b_6/f and cpATPase complexes caused by the loss of the Rieske or ATPase-δ proteins, respectively, complicates the functional analysis of the specific role(s) of the *PetC* and *AtpD* gene products. As a starting point for future functional studies in planta, the *petc-2* and *atpd-1* knock-out mutants generated and characterized in this study should be complemented with mutagenized versions of these proteins that retain the ability to stabilize their multiprotein complexes, while being impaired by mutations at specific sites affecting their specific functions.

MATERIALS AND METHODS

Plant Propagation

Arabidopsis WT (ecotypes Col-0 and L*er*) and mutant plants were grown on Murashige and Skoog medium containing 2% sucrose in a culture chamber on a 16-h-day period (PFD = 12 μmol photons m^{-2} s^{-1}) at 22°C.

Analysis of Nucleic Acids

Arabidopsis DNA was isolated as described by Liu et al. (1995). Total plant RNA was extracted from fresh tissue using the RNeasy Plant System (Qiagen, Hilden, Germany). Northern analyses were performed under stringent conditions according to Sambrook et al. (1989). ^{32}P-labeled probes were derived from the entire coding region of the *AtpD* gene and from the second to fifth exons of the *PetC* cDNA.

Complementation of the *atpd-1* Mutant

The *AtpD* cDNA was ligated into the plant expression vector pPCV702 (Koncz et al., 1990) and introduced into Arabidopsis plants by *Agrobacterium tumefaciens*-mediated transformation as described before (Pesaresi et al., 2001). Successful complementation was confirmed by measuring levels of Chl fluorescence and leaf pigmentation.

Two-Dimensional PAGE and Western Analysis of Proteins

Leaves from 4-week-old plants were harvested in the middle of the light period, and thylakoids were prepared from mesophyll chloroplasts as described by Bassi et al. (1985). For two-dimensional gel analysis, thylakoid membrane samples corresponding to 30 μg of Chl were first fractionated on non-denaturing lithium dodecyl sulfate-PA gradient gels and in the second dimension in a denaturing SDS-PA gradient (10%–16%) gel as described by Pesaresi et al. (2001) and Grasses et al. (2002). Proteins were visualized by Coomassie staining, and densitometric analyses of the protein gels were performed by using the Lumi Analyst 3.0 (Roche Diagnostics, Basel).

For one-dimensional PAGE analysis, amounts of protein equivalent to 5 μg of Chl were loaded for each genotype. Decreasing amounts of WT proteins (3.75, 2.5, and 1.25 μg of Chl) were loaded in parallel lanes (0.75×, 0.5×, and 0.25× WT). For immunoblot analyses, proteins were transferred to Immobilon-P membranes (Millipore, Eschborn, Germany) and incubated with antibodies specific for individual thylakoid polypeptides. Antibodies specific for the following photosynthetic proteins were used: Rieske, cyt b_6, and cpATPase-a and -b (obtained from Lutz Eichacker and Jörg Meurer, Ludwig-Maximilians-Universität, Munich); cpATPase-α and -β (obtained from Alice Barkan, Institute of Molecular Biology, University of Oregon, Eugene, OR); cyt *f* (obtained from Giovanni Finazzi, Institut de Biologie Physico-Chimique); suIV (obtained by Jörg Meurer, Ludwig-Maximilians-Universität Munich and David Stern, Boyce Thompson Institute, Cornell University, Ithaca, NY); cpATPase-δ (obtained from Richard Berzborn, University of Bochum, Germany); PSII-D1 and Lhca4 (obtained from Agrisera, Vännäs, Sweden); and PSI-F (obtained from Poul-Erik Jensen and Henrik Vibe Scheller, The Royal Veterinary and Agricultural University, Copenhagen). Signals were detected using the Enhanced Chemiluminescence Western Blotting kit (Amersham Biosciences, Sunnyvale, CA) and quantified using the Lumi Analyst 3.0 (Roche Diagnostics).

Pigment Analysis

Pigments were analyzed by reversed-phase HPLC (Färber et al., 1997). For pigment extraction, leaf discs were frozen in liquid nitrogen and dis-

rupted in a mortar in the presence of acetone. After a short centrifugation, pigment extracts were filtered through a membrane filter (pore size 0.2 μm) and used directly for HPLC analysis or stored for a maximum of 2 d at 20°C.

Measurements of Chl Fluorescence and the Redox State of P700

In vivo Chl fluorescence of single leaves was excited and detected with a pulse amplitude modulated fluorometer (PAM 101/103, Walz, Effeltrich, Germany). Pulses (800 ms) of white light (6,000 μmol photons m^{-2} s^{-1}) were used to determine the maximum fluorescence (F_m) and the ratio $(F_m - F_0)/F_m = F_v/F_m$. Actinic light with an intensity of 12 μmol photons m^{-2} s^{-1} was used to drive photosynthesis. In addition, photochemical quenching [$qP = (F_{m'} - F_s)/(F_{m'} - F_{0'})$], NPQ [$NPQ = 1 - (F_{m'} - F_{0'})/(F_m - F_0)$], and effective quantum yield [$\Phi_{II} = (F_{m'} - F_{0'})/F_{m'}$] were recorded.

The thylakoid membrane potential decay was measured with an apparatus identical to the one described by Joliot and Joliot (1984). Dark-adapted leaves were exposed to 15-ms (WT) or 25-ms (*atpd-1*) pulses of saturating light to induce a maximum transthylakoid proton gradient. The wavelength was 690 nm, and the intensity corresponded to the transfer of about 4,000 excitations photocenter^{-1} s^{-1}. Under these conditions, a large number of photochemical turnovers were induced and a similar thylakoid membrane potential was reached in the WT and *atpd-1* leaves. The potential reached at the end of the saturating light pulses has been normalized to 10,000. After the light pulse, leaves were kept in the dark, and the thylakoid membrane potential decay was monitored by recording the absorption at 520 nm of short light pulses, weak enough to have no actinic effect (for discussion, see Joliot and Joliot, 2002).

The redox state of P700 under continuous white actinic light was calculated from measurements of changes in P700 absorption at 820 nm with the PAM 101 fluorometer connected to a dual-wavelength emitter-detector unit ED-P700/DW (Walz, Effeltrich, Germany) according to Barth et al. (2001).

Rates of Photosynthetic Electron Transport

Electron transport rates under illumination with saturating actinic light (150 μmol photons m^{-2} s^{-1}) were derived from measurements of photosynthetic oxygen evolution using a Clark-type oxygen electrode (Hansatech Instruments Ltd., Laborbedarf Helmut Sauer, Reutlingen, Germany) at 20°C. Thylakoid concentrations equivalent to 10 μg Chl mL^{-1} were used for all measurements. Linear electron transport ($H_2O \rightarrow K_3[Fe(CN)_6]$) was measured in a medium containing 330 mM sorbitol, 40 mM HEPES/NaOH (pH 7.6), 10 mM NaCl, 5 mM $MgCl_2$, 2 μM gramicidin D, and 5 mM NH_4Cl, using 0.5 mM $K_3[Fe(CN)_6]$ as terminal electron acceptor. PSII activity ($H_2O \rightarrow$ 1,4-benzoquinone) was measured in the same medium using 1 mM 1–4 benzoquinone instead of $K_3[Fe(CN)_6]$ as terminal electron acceptor. PSI activity was measured in 40 mM Tricine/NaOH (pH 8.0), 60 mM KCl, 5 mM $MgCl_2$, 1 mM NaN_3, 1 mM sodium-ascorbate, 100 units of superoxide dismutase, and 1 μM 3-(3–4-di-chlorophenyl)-1,1-dimethylurea, using 0.5 mM 2,3,5,6-tetramethyl-*p*-phenylene-diamine as electron donor and 25 μM methyl viologen as electron acceptor.

Expression Profiling

The 3,292-gene sequence tag nylon array, including 2,661 nuclear chloroplast genes and 631 genes coding for non-chloroplast proteins, each spotted in duplicate, has been described previously (Richly et al., 2003). Total RNA was isolated from 5 g of leaf material obtained from plants at 8-leaf rosette stage (approximately 4-week-old plants). Two independent experiments with different filters, thus considering four (2 × 2) spots for each GST, and independent cDNA probes derived from plant material corresponding to pools of at least 50 individuals of WT or mutant plants were performed, thus minimizing variation between individual plants, filters, or probes. cDNA probes were synthesized by using as primer a mixture of oligonucleotides matching the 3,292 genes in antisense orientation and hybridized to the GST array as described (Kurth et al., 2002; Richly et al., 2003). Images were read using the Storm PhosphorImager (Molecular Dynamics, Sunnyvale, CA). Hybridization images were imported into the ArrayVision program (v6; Imaging Research, Ontario, Canada), where artifacts were removed, background correction was performed, and resulting values were normalized with reference to intensity of all spots on the array (Kurth et al., 2002). In the next step, those data were imported into the ArrayStat program (v1.0 Rev. 2.0; Imaging Research) and a z-test (nominal α set to 0.05) was performed to identify statistically significant differential expression values. Only differential expression values fulfilling the criteria of the z-test are listed in supplementary material 3. Clustering of expression ratios was performed using Genesis Software (v1.1.3; Sturn et al., 2002).

ACKNOWLEDGMENTS

We thank the Salk Institute Genomic Analysis Laboratory for providing the sequence-indexed Arabidopsis T-DNA insertion mutants, and Jörg Meurer and Claudia Nickel for their support in immunoblot analyses. We are grateful to Francis-André Wollman for discussion and critical reading of the manuscript. Grateful acknowledgments are extended to Jörg Nickelsen for his support in tracking the availability of antibodies and to Paul Hardy for critical reading of the manuscript.

Received March 25, 2003; returned for revision April 24, 2003; accepted June 17, 2003.

LITERATURE CITED

Abdallah F, Salamini F, Leister D (2000) A prediction of the size and evolutionary origin of the proteome of chloroplasts of Arabidopsis. Trends Plant Sci **5:** 141–142

Barth C, Krause GH, Winter K (2001) Responses of photosystem I compared with photosystem II to high-light stress in tropical shade and sun leaves. Plant Cell Environ **24:** 163–176

Bassi R, dal Belin Peruffo A, Barbato R, Ghisi R (1985) Differences in chlorophyll-protein complexes and composition of polypeptides between thylakoids from bundle sheaths and mesophyll cells in maize. Eur J Biochem **146:** 589–595

Berry EA, Guergova-Kuras M, Huang LS, Crofts AR (2000) Structure and function of cytochrome *bc* complexes. Annu Rev Biochem **69:** 1005–1075

Böttcher B, Schwarz L, Graber P (1998) Direct indication for the existence of a double stalk in CF_0F_1. J Mol Biol **281:** 757–762

Bruce BD, Malkin R (1991) Biosynthesis of the chloroplast cytochrome b_6f complex: studies in a photosynthetic mutant of Lemna. Plant Cell **3:** 203–212

Budziszewski GJ, Lewis SP, Glover LW, Reineke J, Jones G, Ziemnik LS, Lonowski J, Nyfeler B, Aux G, Zhou Q et al. (2001) Arabidopsis genes essential for seedling viability: isolation of insertional mutants and molecular cloning. Genetics **159:** 1765–1778

Carrell CJ, Zhang H, Cramer WA, Smith JL (1997) Biological identity and diversity in photosynthesis and respiration: structure of the lumen-side domain of the chloroplast Rieske protein. Structure **5:** 1613–1625

Cramer WA, Furbacher PN, Szczepaniak A, Tae G-S (1991) Electron transport between photosystem II and photosystem I. *In* CP Lee, ed, Current Topics in Bioenergetics, Vol. 16. Academic Press, San Diego, pp 179–222

de Vitry C, Finazzi G, Baymann F, Kallas T (1999) Analysis of the nucleus-encoded and chloroplast-targeted Rieske protein by classic and site-directed mutagenesis of *Chlamydomonas*. Plant Cell **11:** 2031–2044

Engelbrecht S, Giakas E, Marx O, Lill H (1998) Fluorescence resonance energy transfer mapping of subunit δ in spinach chloroplast F_1 ATPase. Eur J Biochem **252:** 277–283

Färber A, Young AJ, Ruban AV, Horton P, Jahns P (1997) Dynamics of xanthophyll-cycle activity in different antenna subcomplexes in the photosynthetic membranes of higher plants: the relationship between zeaxanthin conversion and nonphotochemical fluorescence quenching. Plant Physiol **115:** 1609–1618

Grasses T, Pesaresi P, Schiavon F, Varotto C, Salamini F, Jahns P, Leister D (2002) The role of ΔpH-dependent dissipation of excitation energy in protecting photosystem II against light-induced damage in *Arabidopsis thaliana*. Plant Physiol Biochem **40:** 41–49

Groth G, Strotmann H (1999) New results about structure, function and regulation of the chloroplast ATP synthase (CF_0CF_1). Physiol Plant **106:** 142–148

Haldrup A, Naver H, Scheller HV (1999) The interaction between plastocyanin and photosystem I is inefficient in transgenic Arabidopsis plants lacking the PSI-N subunit of photosystem I. Plant J **17:** 689–698

Hazard AL, Senior AE (1994) Defective energy coupling in δ-subunit mutants of *Escherichia coli* F_1F_0-ATP synthase. J Biol Chem **269:** 427–432

Hazard AL, Senior AE (1994) Mutagenesis of subunit δ from *Escherichia coli* F_1F_0-ATP synthase. J Biol Chem **269:** 418–426

Jahns P, Graf M, Munekage Y, Shikanai T (2002) Single point mutation in the Rieske iron-sulfur subunit of cytochrome b_6/f leads to an altered pH dependence of plastoquinol oxidation in Arabidopsis. FEBS Lett **519:** 99–102

Joliot P, Joliot A (1984) Electron transfer between the 2 photosystems: flash excitation under oxidizing conditions. Biochim Biophys Acta **765:** 210–218

Joliot P, Joliot A (2002) Cyclic electron transfer in plant leaf. Proc Natl Acad Sci USA **99:** 10209–10214

Junge W, Rumberg B, Schröder H (1970) The necessity of an electric potential difference and its use for photophosphorylation in short flash groups. Eur J Biochem **14:** 575–581

Kim H, Xia D, Yu CA, Xia JZ, Kachurin AM, Zhang L, Yu L, Deisenhofer J (1998) Inhibitor binding changes domain mobility in the iron-sulfur protein of the mitochondrial *bc*1 complex from bovine heart. Proc Natl Acad Sci USA **95:** 8026–8033

Koncz C, Mayerhofer R, Koncz-Kalman Z, Nawrath C, Reiss B, Redei GP, Schell J (1990) Isolation of a gene encoding a novel chloroplast protein by T-DNA tagging in *Arabidopsis thaliana*. EMBO J **9:** 1337–1346

Kramer DM, Cruz JA, Kanazawa A (2003) Balancing the central roles of the thylakoid proton gradient. Trends Plant Sci **8:** 27–32

Kuras R, Wollman FA (1994) The assembly of cytochrome b_6/f complexes: an approach using genetic transformation of the green alga *Chlamydomonas reinhardtii*. EMBO J **13:** 1019–1027

Kurth J, Varotto C, Pesaresi P, Biehl A, Richly E, Salamini F, Leister D (2002) Gene-sequence-tag expression analyses of 1,800 genes related to chloroplast functions. Planta **215:** 101–109

Lemaire C, Girard-Bascou J, Wollman FA, Bennoun P (1986) Studies on the cytochrome b_6f complex: I. Characterisation of the complex subunits in *Chlamydomonas reinhardtii*. Biochim Biophys Acta **851:** 229–238

Lemaire C, Wollman FA (1989) The chloroplast ATP synthase in *Chlamydomonas reinhardtii*: II. Biochemical studies on its biogenesis using mutants defective in photophosphorylation. J Biol Chem **264:** 10235–10242

Lill H, Hensel F, Junge W, Engelbrecht S (1996) Cross-linking of engineered subunit δ to $(\alpha\beta)_3$ in chloroplast F-ATPase. J Biol Chem **271:** 32737–32742

Liu YG, Mitsukawa N, Oosumi T, Whittier RF (1995) Efficient isolation and mapping of *Arabidopsis thaliana* T-DNA insert junctions by thermal asymmetric interlaced PCR. Plant J **8:** 457–463

Miles D (1982) The use of mutations to probe photosynthesis in higher plants. *In* M Edelman, RB Hallick, N-H Chua, eds, Methods in Chloroplast Molecular Biology. Elsevier Biomedical Press, Amsterdam, pp 75–107

Monde RA, Zito F, Olive J, Wollman FA, Stern DB (2000) Post-transcriptional defects in tobacco chloroplast mutants lacking the cytochrome b_6/f complex. Plant J **21:** 61–72

Muller P, Li XP, Niyogi KK (2001) Non-photochemical quenching: a response to excess light energy. Plant Physiol **125:** 1558–1566

Munekage Y, Takeda S, Endo T, Jahns P, Hashimoto T, Shikanai T (2001) Cytochrome b_6f mutation specifically affects thermal dissipation of absorbed light energy in Arabidopsis. Plant J **28:** 351–359

Pesaresi P, Varotto C, Meurer J, Jahns P, Salamini F, Leister D (2001) Knock-out of the plastid ribosomal protein L11 in Arabidopsis: effects on mRNA translation and photosynthesis. Plant J **27:** 179–189

Pfannschmidt T (2003) Chloroplast redox signals: how photosynthesis controls its own genes. Trends Plant Sci **8:** 33–41

Prescott M, Bush NC, Nagley P, Devenish RJ (1994) Properties of yeast cells depleted of the OSCP subunit of mitochondrial ATP synthase by regulated expression of the *ATP5* gene. Biochem Mol Biol Int **34:** 789–799

Price GD, Yu JW, Voncaemmerer S, Evans JR, Chow WS, Anderson JM, Hurry V, Badger MR (1995) Chloroplast cytochrome b_6/f and ATP synthase complexes in tobacco: transformation with antisense RNA against nuclear-encoded transcripts for the Rieske FeS and ATP-δ polypeptides. Aust J Plant Physiol **22:** 285–297

Richly E, Dietzmann A, Biehl A, Kurth J, Laloi C, Apel K, Salamini F, Leister D (2003) Co-variations in the nuclear chloroplast transcriptome reveal a regulatory master switch. EMBO Rep **4:** 491–498

Robertson D, Woessner JP, Gillham NW, Boynton JE (1989) Molecular characterization of two point mutants in the chloroplast *atpB* gene of the green alga *Chlamydomonas reinhardtii* defective in assembly of the ATP synthase complex. J Biol Chem **264:** 2331–2337

Robinson C, Thompson SJ, Woolhead C (2001) Multiple pathways used for the targeting of thylakoid proteins in chloroplasts. Traffic **2:** 245–251

Sambrook J, Fritsch EF, Maniatis T (1989) Molecular Cloning: A Laboratory Manual, Ed 2. Cold Spring Harbor Laboratory Press, Cold Spring Harbor, NY

Smart EJ, Selman BR (1991) Isolation and characterization of a *Chlamydomonas reinhardtii* mutant lacking the γ-subunit of chloroplast coupling factor 1 (CF_1). Mol Cell Biol **11:** 5053–5058

Smart EJ, Selman BR (1993) Complementation of a *Chlamydomonas reinhardtii* mutant defective in the nuclear gene encoding the chloroplast coupling factor 1 (CF_1) γ-subunit (*atp*C). J Bioenerg Biomembr **25:** 275–284

Stack AE, Cain BD (1994) Mutations in the δ subunit influence the assembly of F_1F_0 ATP synthase in *Escherichia coli*. J Bacteriol **176:** 540–542

Straffon AF, Prescott M, Nagley P, Devenish RJ (1998) The assembly of yeast mitochondrial ATP synthase: subunit depletion in vivo suggests ordered assembly of the stalk subunits b, OSCP and d. Biochim Biophys Acta **1371:** 157–162

Strand A, Asami T, Alonso J, Ecker JR, Chory J (2003) Chloroplast to nucleus communication triggered by accumulation of Mg-protoporphyrin IX. Nature **421:** 79–83

Stubbe W, Herrmann RG (1982) Selection and maintenance of plastome mutants and interspecific genome/plastome hybrids in Oenothera. *In* M Edelman, RB Hallick, N-H Chua, eds, Methods in Chloroplast Molecular Biology. Elsevier Biomedical Press, Amsterdam, pp 149–165

Sturn A, Quackenbush J, Trajanoski Z (2002) Genesis: cluster analysis of microarray data. Bioinformatics **18:** 207–208

Surpin M, Larkin RM, Chory J (2002) Signal transduction between the chloroplast and the nucleus. Plant Cell **14:** S327–S338

Varotto C, Pesaresi P, Meurer J, Oelmuller R, Steiner-Lange S, Salamini F, Leister D (2000) Disruption of the Arabidopsis photosystem I gene *psaE1* affects photosynthesis and impairs growth. Plant J **22:** 115–124

Wisman E, Hartmann U, Sagasser M, Baumann E, Palme K, Hahlbrock K, Saedler H, Weisshaar B (1998) Knock-out mutants from an *En-1* mutagenized *Arabidopsis thaliana* population generate phenylpropanoid biosynthesis phenotypes. Proc Natl Acad Sci USA **95:** 12432–12437